ELSEVIER

Vibrational spectroscopy of gas-phase neutral and cationic phenanthrene in their electronic groundstates

J.A. (Hans) Piest [a,b,*], Jos Oomens [a], Joost Bakker [a], Gert von Helden [a], Gerard Meijer [a,b]

[a] *FOM-Institute for Plasma Physics Rijnhuizen, Edisonbaan 14, NL-3439 BE Nieuwegein, The Netherlands*
[b] *Department of Molecular and Laser Physics, University of Nijmegen, Toernooiveld 1, NL-6525 ED Nijmegen, The Netherlands*

Abstract

Various experimental methods are applied to retrieve the vibrational structure of phenanthrene in its neutral and cationic groundstates. The linear infrared (IR) absorption spectra in the 400–1650 cm^{-1} range of jet-cooled phenanthrene and its cation, both clustered with either an argon or a neon atom, are obtained via photo-induced cluster dissociation spectroscopy. The spectra observed are in good agreement with calculated spectra of the bare species. However, the observed spectrum of cationic phenanthrene shows more lines and lines with different intensities in the 900–1400 cm^{-1} range than expected from calculations. Additional spectra of the perdeuterated phenanthrene–Ar cation, and the warm ($T \gtrsim$ room temperature) bare phenanthrene cation are recorded. Also the mass-analyzed threshold ionization spectra of bare phenanthrene and phenanthrene–Ar are recorded and compared with each other. Comparison of the spectral data recorded to calculated spectra of bare neutral, cationic and cationic perdeuterated phenanthrene, as well as to IR spectra recorded in matrix–isolation experiments, explicitly demonstrates that cluster dissociation spectroscopy is a valid and powerful method to obtain IR spectroscopic information of bare neutral and cationic jet-cooled poly-aromatic hydrocarbons. © 2001 Elsevier Science B.V. All rights reserved.

1. Introduction

In the last decades, poly-aromatic hydrocarbons (PAHs) have been recognized as an important class of molecules in astronomy related spectroscopic problems [1–4]. Besides the diffuse interstellar bands [5–7], a set of absorption features in the visible spectral range, and originating from the interstellar medium (ISM), strong infrared (IR) emission bands, collectively known as the unidentified infrared bands (UIRs) [8], are observed in the emission spectra of a wide range of celestial objects, such as reflection nebulae and planetary nebulae. The most prominent IR emission bands are observed around 3.3, 6.2, 7.7, 8.6 and 11.3 μm, with minor features observed

* Corresponding author. Tel.: +31-24-3652171; fax: +31-24-3653311.

E-mail address: hanspi@sci.kun.nl (J.A. (Hans) Piest).

around 3.4, 5.2, 5.8, 6.8, 7.0 and 12.3 μm. Observation of UIRs in such a wide variety of objects implies simple emission mechanisms only depending on general interstellar environmental conditions, together with an ubiquitous presence of the carriers. Therefore, determining the nature of the UIR-carriers is an important goal in astro-chemistry. Considering the general interstellar conditions (rarefied molecular and dust clouds and cold and collision-free environments), it was shown [1,2] that the UIRs are non-thermal in nature, and most probably originate from very small particles or free molecules that are transiently heated to peak temperatures of ∼1000 K by absorption of a single ultraviolet (UV) photon, and subsequently cool down via emission of IR photons. Although the exact carriers of the IR emission bands are still unknown, it is widely accepted that polycyclic aromatic structures, which normally tend to have IR features around the UIR wavelengths, are likely candidates. Besides carbonaceous structures like coal [9] and quenched carbonaceous composites [10–12], free PAHs, either neutral or ionized, are proposed as important candidates [2,3,13]. In general, PAHs are moderately stable in their neutral and singly ionized forms in the ISM. High internal energies are needed to destruct PAHs [14–18], therefore, photoexcited neutral and singly ionized PAHs of any size prefer to relax by IR emission. Considering the UV fluxes in planetary and reflection nebulae, and HII regions, it is assumed from model calculations that it takes PAHs of at least ∼50 carbon atoms to reach stability against UV absorption [4,19,20]. However, recent experiments on 23 PAHs and C_{60} have shown that among the smaller PAHs photostable species exist, whereas all species with larger masses show evidence of photofragmentation [21]. In order to draw firm conclusions on the PAH hypothesis, relevant laboratory data are needed. Only few laboratory experiments regarding PAHs under conditions similar to the ISM have been conducted. The ideal experiment should involve IR emission spectroscopy after absorbing a single UV photon by a cold neutral or ionized PAH in the gas phase. However, due to the fairly long IR radiation lifetimes (∼ms) this is a very difficult experiment.

Only with the use of an extremely sensitive IR detector, capable of detecting single IR photons, it has been possible to record the IR emission spectra of several neutral PAHs, sizing up to coronene ($C_{24}H_{12}$), this way [22,23]. These studies confirmed the widely accepted assumption that neutral PAHs of small and moderate sizes can at best make a minor contribution to the UIRs [3,4]. Larger neutral PAHs and PAHs in their cationic form, still remain viable candidates [24–26].

Other methods used to obtain IR spectral data of PAHs are based on absorption rather than emission of IR photons. Although the IR absorption spectrum of a cold PAH is not trivially the same as that of a transiently heated, rotationally and electronically cold and vibrationally hot PAH, these absorption spectra still hold important information on fundamental IR optical properties like positions and (relative) intensities of fundamental IR modes, possibly leading to improved IR emission models.

In the last decade, a comprehensive database of IR spectra of PAHs and their cations has been constructed via matrix–isolation (MI) spectroscopy [13,24,25,27–40]. In this method, neutral PAHs are deposited in noble gas matrices with temperatures of ∼10–20 K, and their direct IR absorption spectrum is analyzed with a Fourier transform IR spectrometer. Since no species selectivity is involved, the IR spectrum recorded is the sum of that of all species deposited in the matrix making correlation measurements necessary. Recording the PAH cationic IR spectrum is accomplished by in situ photolysis of neutral molecules using an UV-lightsource. Typically, a fraction of up to 10% of the neutral PAHs is ionized. A serious limitation of MI spectroscopy of cations is confusion with residual neutral PAH bands, making the spectra difficult to interpret. To distinguish PAH cation bands, a variety of methods are used. Enhancement in the presence of an electron acceptor, correlation with known UV/visual band intensities, correlation in the growth and evolution of the IR bands under photolysis, correlation of band intensities with ionization efficiency and comparison to theory are important ways to determine the cationic spectrum. Other potential problems of MI spec-

troscopy, applied to ions, are shielding of ionic absorption bands by intense neutral bands and unknown matrix-interaction possibly adding shifts to line positions and changes in line intensities.

Therefore, it is desirable to conduct IR spectroscopy of PAHs in the gas phase, for instance in the collision-free environment of a molecular jet, in combination with a species selective detection scheme. Throughout the years, a large amount of vibrational spectroscopic data of neutral and ionized species have been collected using molecular jets (see [41] for an overview). However, reports on true IR spectra of aromatic molecules and ions in a molecular jet are scarce, mainly due to the relatively small populations of cold species that can be generated in such jets, together with a lack of bright and tunable lightsources in the IR wavelength range. We have been experimenting with a free electron laser (FEL), which produces bright and continuously tunable IR radiation, combined with a molecular beam spectrometer [41–44]. In this system, high laserfluences combined with the relatively small populations of molecules of interest and short pathlengths make direct absorption spectroscopic methods unfavorable. Instead, sophisticated detection methods, taking advantage of the inherently high sensitivity of ion counting are applied to retrieve molecular vibrational spectra.

In this paper, we report the results of molecular beam experiments, in which the IR spectra of neutral, cationic and perdeuterated cationic phenanthrene clustered with argon (also neon in the case of ionic phenanthrene) are recorded via IR induced cluster dissociation. The method used is similar to that used for obtaining electronic spectra of cationic PAHs [45,46].

Additional IR and vibrational spectroscopic data of bare ionic phenanthrene is obtained via IR induced photo-fragmentation at temperatures around room temperature, and via mass-analyzed threshold ionization (MATI) spectroscopy of the cold neutral bare molecule. For jet-cooled bare neutral phenanthrene IR-UV two color resonant enhanced multiphoton ionization (IR-UV-REMPI) is applied in a similar scheme as is earlier used on other molecules [47,48]. All spectra are compared with MI data recorded by others[34,37,49].

The first experiments of IR induced cluster dissociation spectroscopy were conducted in the mid '80s[50]. In these experiments protonated hydrogen clusters (H_3^+-$(H_2)_n$) were irradiated with IR light. IR transitions of the parent cluster were detected by loss of a H_2 unit after absorbing resonant IR photons. In follow up experiments also the spectra of H_3O^+-$(H_2O)_n$-$(H_2)_n$ clusters were recorded [51]. This early work mainly focused on the IR spectroscopy of the clusters and not on that of the bare ions. Intensities and line positions of the cluster change significantly between clusters of different sizes, due to strong interaction of H_2 and H_2O molecules with the small ionic core. Experiments with larger neutral and ionic moieties, such as $C_6H_6(H_2O)_n$ [52], CH_3CNH^+–H_2 [53], and $C_6H_5OH^+$–$(H_2O)_n$ [54] already show much smaller line shifts. Ultimately, in experiments with large molecules, such as aromatic species, clustered with noble gas atoms, vibrational line shifts and intensity changes become almost negligible [48,55]. Spectroscopy of, for instance, anthracene in the neutral S_1 state using laser induced fluorescence spectroscopy [56], or naphthalene [57] in its ionic groundstate using zero kinetic energy spectroscopy, showed that line shifts are normally limited to a few wavenumbers, and intensities mimic those of the bare species. This is also indicated by the fairly small line shifts and intensity changes between data recorded via cluster dissociation of the naphthalene–Ar cluster cation compared to observed spectra of matrix–isolated cationic naphthalene [42].

Only in exceptional cases, when individual modes are unusually strongly coupled to the Van der Waals vibrational modes, anomalous shifts are observed [58]. The largest known shift of 26.5 cm^{-1} is observed in the $16a^2$ overtone, which is observed at 380 cm^{-1} of aniline–Ar. From these experiments, it is also known that anomalous shifts depend strongly on the type of noble gas atom and, therefore, can be revealed by observing spectra using different noble gases.

The steadily increasing IR database, formed by earlier work in the 3000 cm^{-1} region by others and in the 400–1700 cm^{-1} region, together with the newly observed data explicitly demonstrate that cluster dissociation spectroscopy is a power-

ful method to obtain IR spectral data of bare neutral and cationic jet-cooled PAHs [41–44,48,55].

2. The free-electron laser for infrared experiments (FELIX)

All experiments are carried out at the user-facility 'Free-Electron Laser for Infrared Experiments' (FELIX) at the FOM-institute for Plasmaphysics Rijnhuizen, Nieuwegein, the Netherlands[1] [59,60].

In FELIX, free (unbound) electrons, generated by an electron-gun, are accelerated to highly relativistic speeds by linear accelerators, before injecting them into the FEL-cavity. After entering this cavity, electromagnetic radiation is generated by providing a spatially periodic magnetic field, with period λ_u, and strength B_u, with an undulator. This magnetic field induces a periodic modulation of the transverse velocity of the electrons resulting in emission of synchrotron radiation. Being captured in the cavity, radiation with wavelength λ_0, fulfilling the FEL-resonance condition, $\lambda_0 = \lambda_u [1 + \alpha^2 B_u^2]/2\gamma^2$, will be selectively amplified on successive cavity roundtrips by interaction with newly injected electrons. In this formula, γ and α represent the Lorentz factor and a constant proportional to λ_u and inversely proportional to the electron equivalent restmass, respectively. Thus, wavelength tuning can be accomplished by either changing the beam energy ($\sim \gamma$) or the magnetic field strength B_u. With application of both methods, FELIX is capable of producing continuously tunable IR light pulses in the 40–2500 cm^{-1} range, with a typical power of several tens of mJ per pulse and a typical duration of several microseconds. Each of these so-called 'macropulses' has a substructure of pico-second 'micropulses' directly reflecting the pattern of the electron-bunches traveling through the FEL-cavity. With the macropulse energy distributed among the micropulses, the high peak intensities in these micropulses allow for non-linear IR spectroscopy. The spectral width of a single micropulse is al-

most transform limited, i.e. the product of pulse duration and spectral width is close to the minimum given by the Heisenberg uncertainty relation. The micropulse duration can be varied from 6 to 100 optical cycles, corresponding to a spectral width of 7–0.4% FWHM (full width at half maximum) of the central wavelength. In the cluster-dissociation experiments carried out the spectral width selected is typically $\sim 0.5\%$.

3. Infrared spectroscopy of jet-cooled phenanthrene and its cation

A standard molecular beam setup is used to generate a supersonic molecular jet, containing gas phase neutral phenanthrene as well as its Van der Waals cluster. The molecules are resonantly excited to specific electronically excited states using UV photons generated with a Nd:YAG-pumped dye laser system. IR spectroscopy is being carried out using light generated by FELIX. To support the cluster dissociation spectra observed, MATI spectra and IR-UV-REMPI spectra are recorded as well. The spectra recorded are compared with calculated IR spectra of bare neutral and cationic phenanthrene.

3.1. Jet-cooling mass spectrometer

The jet-cooling mass spectrometer used in these experiments has been described more extensively in an earlier paper [61]. In short, the spectrometer consists of two Nd:YAG-pumped dye lasers, a molecular beam generator and a time-of-flight detection unit.

The Spectra Physics PDL2 and PDL3 dye lasers are separately pumped by the frequency doubled outputs (532 nm) of a Spectra Physics GCR-11 Nd:YAG laser and a Spectra Physics GCR-150 Nd:YAG laser, respectively. The dye laser fundamentals are frequency doubled by KDP crystals before being co-aligned using a beamcombiner and being coupled into the molecular beam apparatus. The IR FELIX-beam enters the molecular beam apparatus, counterpropagating to the dye laser beams, via a vacuumline.

---

[1] http://ns2.rijnh.n1/n4/f1234.htm.

The molecular beam is generated using a pulsed supersonic valve (R.M. Jordan Co.). Phenanthrene is put in the sample compartment of this valve, which is kept at a temperature of 75°C, to provide a sufficient vapor pressure. Argon at a stagnation pressure of 2.5 bar is used as carrier gas. Gas-pulses with a duration of around 50 μs are released into a vacuum of 10^{-6} Torr. In the expansion, the internal energy of the sample molecules is transferred to the carrier gas atoms, yielding molecules in their vibronic groundstates, which allows for formation of, weakly bound, Van der Waals clusters.

Upon entering the differentially pumped time-of-flight (TOF) detection unit the molecular beam is skimmed by a slit-skimmer 4 cm downstream the pulsed valve. The background pressure in this detection unit is kept around 10^{-7} Torr, providing essentially collisionfree conditions in the TOF region. The TOF detector used is a linear orthogonal Wiley–McLaren type TOF setup [62], as is depicted in Fig. 1. At the crossing point of the mutually orthogonal molecular beam axis, the laser beam axis and the TOF drift-tube axis, in between the lower two of three grids of the TOF extraction unit, the species of interest is excited and ionized by the dye lasers using two-color resonant enhanced multi-photon ionization ((1 + 1′) REMPI) via a selected intermediate electronic state (normally the S_1, state). When ionization takes place, the electrical potentials of the two lower grids are kept the same (around 3 kV) yielding field-free ionization conditions. Several microseconds after the ionization, application of

an additional 400 V pulse extracts the ions to the region in between the upper two grids to be further accelerated by a 3 kV/cm electric field. The ions are detected using a micro-channel-plate detector mounted at the end of a 60 cm TOF drift-tube. In this setup, the flight time t_f of an ionized species (mass m, charge q) is proportional to $t_f \sim (m/q)^{1/2}$. Thus, when feeding the detector signal to a 10 bit digital oscilloscope (LeCroy 9430), mass-selective detection with a mass-resolution of around $m/\Delta m \sim 200$ can be achieved by observing signals at specific flight times. The signals are stored on a personal computer that is also used to control the wavelength scanning of the FEL.

3.2. Detection schemes

Recording of the IR spectra of either the neutral groundstate, or the ionic groundstate of phenanthrene–Ar is carried out by application of one of the two excitation schemes that are shown in Fig. 2.

To obtain the IR spectrum of neutral groundstate phenanthrene, clustered with argon, the cluster in the groundstate is irradiated by the IR laser before being excited resonantly via the S_1-state (29 314 cm^{-1}) [63]. The corresponding transition in bare phenanthrene is observed at 29 326 cm^{-1} [63], thus bare phenanthrene is not excited resonantly. After excitation the cluster is ionized to its ionic groundstate by the second UV laser at $\sim 34\ 275$ cm^{-1}. Setting the ionization photon energy to a value just above the ionization threshold (IP) of the cluster avoids dissociation directly after ionization. If the IR laser is resonant with an IR transition in the electronic groundstate, dissociation of the neutral cluster is detected as depletion of the phenanthrene–Ar ion intensity, resulting in the IR spectrum of the neutral species.

In an additional experiment, bare phenanthrene in its neutral groundstate is irradiated with IR light of FELIX and subsequently irradiated with UV light of a F_2 excimer laser, which scheme is depicted in the right panel of Fig. 3. This scheme is similar to the one used in a former experiment on warm *p*-amino-benzoic-acid [47], and to that

extracted ions
to MCP–detector

phenanthrene
+ argon

pulsed valve

skimmer

+3 kV
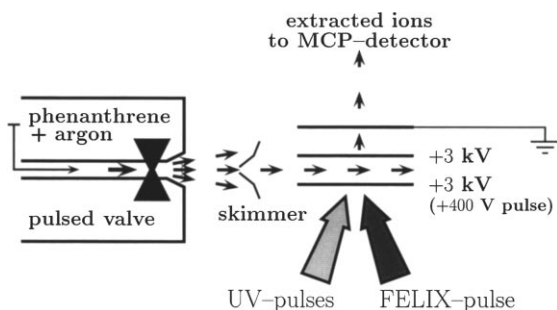+3 kV
(+400 V pulse)

UV–pulses   FELIX–pulse

Fig. 1. Schematic picture of the molecular beam source in combination with the Wiley–McLaren type time-of-flight setup.
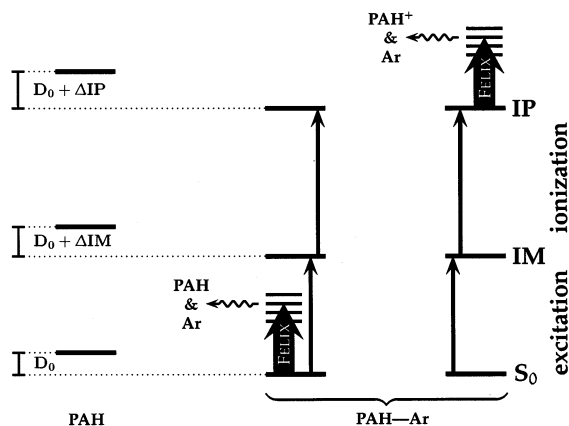
Fig. 2. Dissociation schemes used to record the IR spectra of a groundstate (S_0) neutral PAH–Ar cluster (middle) and that of a groundstate ionized cluster (right). On the left, the energy level diagram of the bare PAH is depicted. Soft ionization to barely above the ionization threshold (IP) of the Van der Waals cluster yields the time-of-flight signal of the cluster ion alone. Following absorption of IR photons before UV excitation, via a selected intermediate state (IM), dissociation of the cluster in its neutral groundstate leads to depletion of the cluster ion signal, which is recorded as function of the IR wavelength. In case of the ionic cluster, IR absorption and subsequent cluster dissociation is induced after UV ionization. Then, not only depletion of the cluster ion signals the presence of an IR resonance, but more important, the appearance of the bare PAH ion signal in the TOF-spectrum signals the presence of resonances against zero background.

used to obtain IR spectra of *p*-ethylphenol and its argon Van der Waals cluster [48].

The ionization threshold of bare phenanthrene at $\sim 63\,654$ cm^{-1} is a little higher than the energy of the two UV lines (63 450 and 63 483 cm^{-1}) [47] produced by the F_2 excimer laser. Therefore, only if the IR laser is resonant with an allowed IR transition and IR photons are absorbed, ionization with the excimer laser can take place. Scanning the FEL over the IR manifold of the neutral groundstate yields the two color IR-UV-REMPI spectrum of bare neutral phenanthrene. It should be noted that the intensities observed via this method are not necessarily the same as those observed in the true IR spectrum. The IR-UV-REMPI intensities depend on the product of the IR absorption cross-section with the absorption cross-section of the ionization step. The latter does not have to be large in a cold

molecule if ionizing from a neutral groundstate vibrational level to ionic groundstate vibrational levels and may also depend on the initially excited vibrational mode of the neutral groundstate molecule. Therefore, intensities are difficult to interpret. However, line positions should be the same as those observed in the true IR spectrum.

Following the scheme depicted in the right panel of Fig. 2, the IR spectrum of the ionic phenanthrene–Ar Van der Waals cluster is obtained. Detection of the IR resonances is accomplished by recording the TOF-signals of both the cluster-ion and the bare ion simultaneously. Using a scheme similar to that which is used to obtain UV spectral data of PAH cations [45,46], phenanthrene–Ar Van der Waals clusters are resonantly ionized to barely above their ionization threshold. At resonances of the ionic cluster, dissociation to a neutral argon atom and bare ionic phenanthrene follows absorption of IR photons. Detection of the bare ion signal against zero background and normalization of the signal to the total amount of cluster-ions produced directly after UV-excitation yield an IR spectrum of the ionic Van der Waals cluster with a high signal-to-noise ratio (SNR).
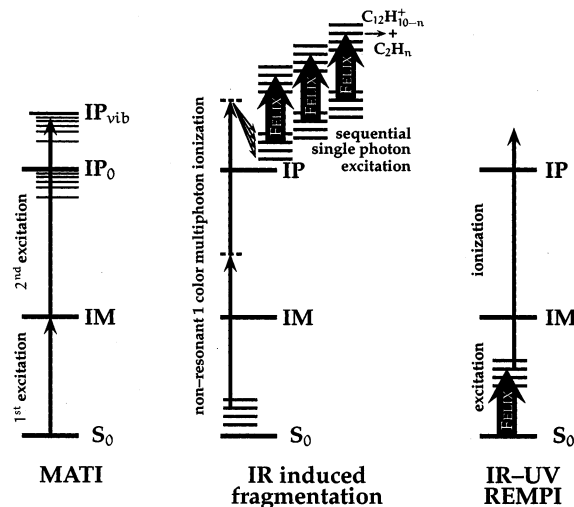

Fig. 3. To obtain additional vibrational data of bare phenanthrene either the MATI spectrum (left), the photo-induced fragmentation IR spectrum of the ion (middle), or the IR-UV REMPI spectrum of neutral phenanthrene (right) is recorded.

Additional information about the vibrational energy-levels of the ionic bare molecule and its Van der Waals cluster can be obtained using MATI spectroscopy. Using the MATI method highly excited Rydberg levels of the neutral molecule, that are present just below the ionic energy levels, are detected in order to reveal the ionic vibrational structure [64]. In contrast with all other experiments carried out, no IR light-source is needed for doing MATI spectroscopy. In MATI, the ionization laser is scanned over the energy-levels of the ion, as is depicted in the left panel of Fig. 3. According to the Rydberg formula $E_{neutral} = E_{ion} - (Z^2 R_M)/(n - \delta_l)^2$, a Rydberg series of metastable states of the neutral species converges to the energy-levels of the cation. In this formula, $E_{neutral}$ and E_{ion} refer to the neutral and ionic energy levels, respectively. Further, Z, R_M, n and δ_l refer to the core charge, the Rydberg-constant for the particular molecular mass M, the principal quantum number, and the quantum defect belonging to the angular momentum state l, respectively. When scanning the UV laser over the high Rydberg manifolds of the neutral molecule, direct ions and highly excited Rydberg neutrals are produced. Shortly (~ 50 ns) after the ionization laserpulse, the application of a small electric field of 2 V cm^{-1} results in a spatial separation of the direct ions and the Rydberg neutrals. The polarity of the small electric field is chosen such that the direct ions move towards the middle grid of the TOF-detector. After ~ 10 μs, the Rydberg neutrals are field ionized and extracted by the regular 400 V extraction pulse. A long time-delay between UV-excitation and pulsed field extraction is necessary mainly for two reasons — (1) to provide a sufficient spatial separation of the direct ions and the Rydberg neutrals; and (2) the lifetime of a high Rydberg state strongly increases with increasing quantum number n [65–67], thus, with a long time-delay, only the highest Rydberg states just below the ionic energy level belonging to that particular Rydberg series, survive and can be detected after field ionization and extraction. Due to the spatial separation the direct ions gain less energy with respect to the middle TOF grid then the field-ionized MATI ions. Detection of these MATI ions after

field-ionization and extraction yields the position of the energy levels of the ion. Background free detection is accomplished using a reversed electric field in front of the MCP detector, which is adjusted such that the direct ions are bent away from the MCP detector, whereas the MATI ions have sufficient energy to pass this reflector and are detected subsequently.

MATI spectroscopy gives information about the position of the energy levels of the ion, however, no stringent selection rules apply between transitions of the S_1 state and the highly mixed, high Rydberg states, therefore, intensities in the MATI spectrum are difficult to interpret.

4. Infrared spectroscopy of the trapped warm phenanthrene cation

Bare phenanthrene cations localized in an ion trap can be fragmented when exposed to the intense IR radiation field of the focused output of FELIX, if tuned to an IR allowed transition of the ion. Due to the high density of vibrational states in species of this size, intramolecular vibrational redistribution (IVR) typically takes place on the sub-ns timescale [68]. Provided transition dipole moment and laser fluence are large enough, the ions reach internal energies above their fragmentation threshold by sequential photon absorption during a FELIX macropulse. The dissociation rate depends on the internal energy and can easily become comparable to or faster than collisional and radiative decay rates [69].

4.1. Ion trap experimental setup

The experimental apparatus has been described in detail in a recent paper [70]. Briefly, a Paul type quadrupole ion trap [71] (R.M. Jordan Co.) is made accessible to ionization and fragmentation laser beams as depicted in Fig. 4.

The toroidal ring electrode has an inner diameter of 2 cm and is fed with a 1 MHz RF voltage of ~ 1000 V peak–peak. At the center of this electrode, vapor phase neutral phenanthrene at room temperature is ionized by the focused 193 nm output of an ArF excimer laser and is instantaneously trapped.
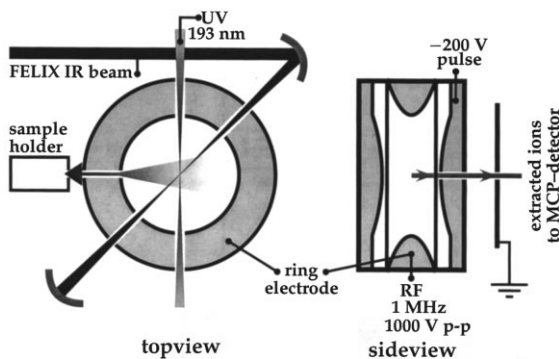
Fig. 4. Scheme of the photo-fragmentation setup used.

Shortly after the UV pulse, the RF amplitude is slightly increased for a short period of time, in order to eject contaminant fragments, induced by the excimer laser, from the trap. Thus, the phenanthrene cation is the lightest species trapped and the fragmentation products, induced by the focused IR laser, can be detected and analyzed against zero background via TOF mass spectrometry ($m/\Delta m \sim 50$). The relevant excitation scheme is depicted in the middle panel of Fig. 3. Typically, the fragments produced by a few subsequent macropulses are collected in the trap before being extracted by application of a 200 V voltage dip to the endcap electrode nearest to the MCP-detector. The MCP transient is captured by a 10 bit digital oscilloscope (LeCroy 9430). The fragment ion yield is recorded at the C_2H_n-loss channel [21].

5. Results

The resulting spectra of IR cluster dissociation spectroscopy applied to cationic phenanthrene clustered with argon and with neon, together with those of perdeuterated cationic phenanthrene clustered with argon are presented. Additional information on vibrational modes of bare ionic phenanthrene is presented via a MATI spectrum, and via an IR induced fragmentation spectrum. The cluster dissociation spectrum of neutral phenanthrene is presented together with that of the IR-UV-REMPI spectrum of bare neutral phenanthrene. All spectral data are tabulated in Table 1

(phenanthrene ionic data), Table 2 (perdeuterated phenanthrene ionic data), and Table 3 (neutral phenanthrene data), and compared with literature spectra [34,37,49], and calculated spectra implementing the B3LYP method using Dunning's D95(d,p) basisset [72] with Gaussian 98 [73].

5.1. Cationic phenanthrene

Using the methods described earlier, the IR spectrum of phenanthrene clustered with an argon atom in its ionic groundstate is recorded. In Fig. 5, the spectrum observed is compared with a calculated spectrum of bare cationic phenanthrene. In this calculation, which is in reasonable agreement with formerly presented calculations [74], the stick-spectrum is convoluted with a 5 cm^{-1} FWHM Gaussian. Compared with the observed spectrum the 400–900 cm^{-1} range and the 1400–1700 cm^{-1} range are reproduced well by calculations. In these ranges, the calculated lines appear to be blue-shifted on the order of a few percent ($< 3\%$). Also the relative line intensities agree well with those observed. However, in the 900–1400 cm^{-1} region major discrepancies exist between the observed and the calculated spectra. In the spectrum recorded, more lines with different intensities than expected from the calculations are observed. The calculated lines in this region also show unusual large blue shifts.

To check the quality of our calculations, additional computations at the B3LYP level are carried out, using the 4–31g, 6–31g, 6–31g* and 6–31g** basissets. The spectra yielded for the bare phenanthrene cation using either the 6–31g* or the 6–31g** set are practically identical to the D95(d,p) spectrum. Surprisingly, if using either the 4–31g or the 6–31g set, the two smallest basissets of the sets used, the calculated line positions seem to match the observations slightly better in the 900–1400 cm^{-1} spectral region. Still even then, more lines and lines with different intensities are observed than expected from calculations.

The differences between calculations using either the 4–31g/6–31g basissets or using the 6–31g*/6–31g**/D95(d,p) basissets are not in agreement with earlier reported differences between the

Table 1
Frequencies of cationic phenanthrene observed via photo-induced cluster dissociation of phenanthrene–Ar and phenanthrene–Ne compared with MI data (Hudgins), the IR induced photo-fragmentation data of warm cationic phenanthrene, and the MATI data of bare phenanthrene and that of phenanthrene–Ar. Also tabulated are frequencies and integrated IR absorption intensities obtained by calculations[a]

Irrep.	Ph–Ar	Ph–Ne	MI[b]	Warm	MATI		Calc.	
					Ph	Ph–Ar		
C_{2v}	ν_{vib} cm^{-1}	ν_{vib} cm^{-1}	ν_{vib} cm^{-1}	ν_{vib} cm^{-1}	ν_{vib} cm^{-1}	ν_{vib} cm^{-1}	ν_{vib} cm^{-1}	Int./km mol^{-1}
A1	1623						1644	18.7
B2	1571		1565 cmplx	1540			1606	218.8
A1	1558		1558.6				1585	115.2
–	1535		1551.4					
B2	1521		1513.4				1554	11.9
–	1488							
B2	1447			1443			1464	65.4
B2	1434		1432.0				1450	19.6
A1	1423						1443	4.5
–	1345							
–	1292	1294	1299.4					
–	1275	1276	1277.8/1283.0	1259				
–			1264.9/1267.4					
–	1257	1262	1258.9	1228				
–	1228	1231						
–	1216	1220						
–	1201	1203						
–	1177	1176						
–	1138	1139	1136.6/1139.8	1129				
–	1123	1123	1129.9					
–	1095	1096	1096.6/1102.9					
–	1063	1064						
–	1036	1036	1042.1	1034				
–	1018	1019						
–	997	997						
–	985	985		985				
–	969	968						
–	882	883		874				
–	872	872						
–	855	855		838				
B1	835	836	836.2	826			859	45.3
A2					780		792	
B1/A2					759		777/778	
B1	756	755	756.3	744			777	57.8
A1/B1/B2					702		708/711/715	
B1	695	694	694.9	684			711	41.4
A1/A2					615*			
B2	581	580	582.5	578	575		591	45.3
A1/A2					541		546/551	
B2	482				480		487	3.1
B1					465		478	
B2					402		433	
B1					398		414	
Al					372		403	
A2					366		383	
A1/A2					305**			
A2/A1					239	239	238/240	
B1					96		105	
A2					78	80	84	

[a] *239 + 372 combination band (tentative). **78 + 239 combination band (tentative). –, not assigned.
[b] [49].

Table 2
Frequencies of perdeuterated cationic phenanthrene observed via photo-induced cluster dissociation, compared with MI data (Hudgins). Also tabulated are the calculated frequencies and integrated IR absorption intensities[a]

Irrep.	Ph$_{d10}$–Ar	MI[b]	Calc.	
C_{2v}	ν_{vib} cm^{-1}	ν_{vib} cm^{-1}	ν_{vib} cm^{-1}	Int./ km mol^{-1}
A1	1547	1547.0	1616	9.9
B2	1522	1525.9/1528.0	1569	279.9
A1	1506	1507.0	1542	94.3
B2	1455	1459.5	1489	57.5
–	1405	1400.3		
B2	1342	1344.2	1365	36.2
–	1227	1230.4		
B2	1220	1221.5	1322	96.3
–	1214	1213.5		
–	1202	1201.6		
B2	1194	1194.1	1284	186.8
–	1174	1176.6		
–	1158			
–	1136			
–	1110	1114.8		
–	1082			
–	1056			
–	1050			
–	1022			
–	1017			
–	1012	1013.4		
–	995			
–	971			
–	961	958.5		
–	953			
–	894			
–	864			
–	855	856.2		
–	844			
–	829			
–	799			
B1	749		765	2.8
B1	660		677	14.5
B1	612		628	1.1
B1	565	566.7	579	45.5
B2	562		572	36.0
B2	455		461	3.1
B2	400		406	0.3
B1	349		361	12.8

[a] –, not assigned.
[b] [34].

4–31g and 6–31g* basissets for calculated spectra of other PAH cations[74]. For these other PAH cations, the 4–31g and 6–31g* basis- sets yielded similar spectra with essentially only different blueshifts. Increasing the basisset from 4–31g to 6–31g, and the addition of d- and p-functions to the basisset changes the spectra calculated for the phenanthrene cation in the 1050–1500 cm^{-1} region significantly. An explanation for this behavior probably needs a deeper theoretical study.

To address the unexpected behavior in the spectrum observed, the spectrum of cationic phenanthrene clustered with a neon atom is recorded in the $575–1350$ cm^{-1} range. The Van der Waals bond energy of the phenanthrene–Ne cluster is less than that of the phenanthrene–Ar cluster. Also, the mass of neon is only half that of argon. Therefore, with an electronic shift of only 2 cm^{-1} (12 cm^{-1} in the argon cluster) upon excitation via the S_1-state and an increased bond energy of only 28 cm^{-1} (65 cm^{-1} in the argon cluster) in the ionic groundstate with respect to the neutral groundstate, a weaker interaction between the neon atom and the phenanthrene chromophore in the ionic groundstate is expected. For that reason, the ionic phenanthrene–Ne spectrum should resemble the spectrum of bare cationic phenanthrene better. The spectrum observed is presented in the upper panel (lower trace) of Fig. 5. Comparing the cationic phenanthrene–Ne spectrum to that of phenanthrene–Ar, it is clearly seen that within experimental errors, all lines are reproduced at the same positions and with the same relative intensities. Minor shifts (< 5 cm^{-1}) to the blue appear in the 1200 cm^{-1} band. Noting that the frequency calibration of the FELIX output in this region is at best 0.1% (~ 1.2 cm^{-1})

of the central frequency, the agreement between the spectrum of cationic phenanthrene clustered with argon and that of phenanthrene clustered with neon is very good.

Additionally, the spectrum of cationic perdeuterated phenanthrene clustered with argon is recorded. This spectrum is presented, together with the calculated spectrum of the bare perdeuterated cation, in Fig. 6. Again, good agreement with calculations exists in the $400–800$ cm^{-1} and the $1300–1600$ cm^{-1} regions, whereas the $800–1300$ cm^{-1} region shows additional peaks. In the low frequency region, the double peak observed at 562 and 565 cm^{-1} is reproduced well by the calculations. Observation of the dependence of line intensities on the IR fluence, show a linear behavior of the 455 cm^{-1} mode and a higher than linear behavior of the 349 cm^{-1} mode.

In an attempt to clarify the unexpected behavior of the observed ionic spectra in the 1000 cm^{-1} region, the MATI spectrum of bare neutral phenanthrene, yielding information about the vibrational energy levels of the cation, is recorded in the $0–800$ cm^{-1} range above the IP. Coincidences with broad features of the strong $S_2 \leftarrow S_0$ band ($\sim$ 35 386 cm^{-1}) [75] of neutral phenanthrene,

Table 3
Frequencies of neutral phenanthrene observed via photo-induced cluster dissociation and IR-UV-REMPI compared with MI data (Hudgins). Also tabulated are the calculated frequencies and integrated IR absorption intensities

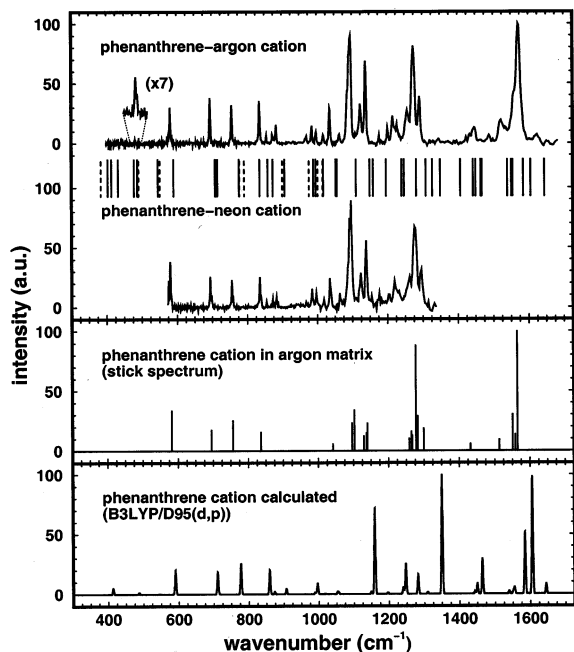| Irrep.	Ph–Ar	IR-UV-REMPI	MI[a]	Calc.	
C_{2v}	ν_{vib} cm^{-1}	ν_{vib} cm^{-1}	ν_{vib} cm^{-1}	ν_{vib} cm^{-1}	int./km mol^{-1}
A1	1304		1302.9	1328	2.5
A1	1251		1245.8/1250.6	1265	11.2
B2	1041		1039.9/1044.3	1054	7.6
B2	1001		1002.5/1003.7	1009	2.3
B1	948		948.2	966	5.6
B1	876		877.6	887	18.6
B2	864		864.9	883	2.3
B1	812	812	812.8	835	59.7
B1	735	734	735.0	752	97.5
B1	714		714.5	733	2.1
B2	710		710.2	720	2.2
B2	618		617.5/618.8	623	6.2
B1	511			512	5.1
B2	493		494.0	500	0.8
B1	424			438	8.5

[a] [37].

Fig. 5. Spectra of cationic phenanthrene clustered with argon (upper panel, upper trace) and clustered with neon (upper panel, lower trace) compared with a stick spectrum of the MI cation (middle panel) as obtained by Hudgins and coworkers, and the calculated spectrum of the cation of bare phenanthrene (lower panel). Between the spectra of the argon and the neon cluster fundamental vibrational frequencies are depicted. Solid bars indicate IR allowed transitions to modes of A1, B1, and B2 symmetry. Dotted bars indicate the IR forbidden transitions to modes of A2 symmetry.

caused by one color REMPI of the ionization laser alone, hindered reliable spectroscopy at frequencies above 800 cm^{-1}. However, in the 0–800 cm^{-1} range, a clean MATI spectrum is observed, which is shown in the middle and upper panel of Fig. 7. Comparison with the calculated line positions show that the strongest bands besides the groundstate peak are positioned at modes of A1 and A2 symmetry and at positions, where fundamental modes are close together. The MATI spectrum of the phenanthrene–Ar Van der Waals cluster is recorded in the 0–250 cm^{-1} region and presented in lower panel of Fig. 7. It shows two bands at 80 and 239 cm^{-1} besides the ionic groundstate, respectively. The corresponding region of the bare species also shows these two bands at 78 and 239 cm^{-1} with similar relative intensities.

In addition to the experiments on jet cooled cationic phenanthrene, the warm IR spectrum of the bare phenanthrene cation is recorded using the photo-fragmention method described earlier and compared with the spectrum obtained via cluster dissociation of the phenanthrene–Ar cation. The results are shown in Fig. 8.

It is observed that band intensities show a non-linear dependence on the IR fluence and that different bands scale differently with increasing fluence. Therefore, correcting to first order, only a linear correction for IR fluence is applied. The spectrum of warm cationic phenanthrene shows an expected agreement with that of jet-cooled cationic phenanthrene–Ar, i.e. with broadened bands shifted to the red compared with those of the jet-cooled cation [76]. The low frequency bands in the 600–1000 cm^{-1} range are all present. The extra peaks, unexpected from calculations, around 1000 cm^{-1} appear in the warm spectrum as a plateau. Three of the four prominent peaks observed at 1138, 1275 and 1571 cm^{-1} in the cluster spectrum, are also present in the warm cationic spectrum at 1129, 1259, and 1540 cm^{-1}, respectively. However, the fourth strong band, observed at 1095 cm^{-1} in the cluster dissociation spectrum, seems to be much less prominent in the spectrum of the warm cation.
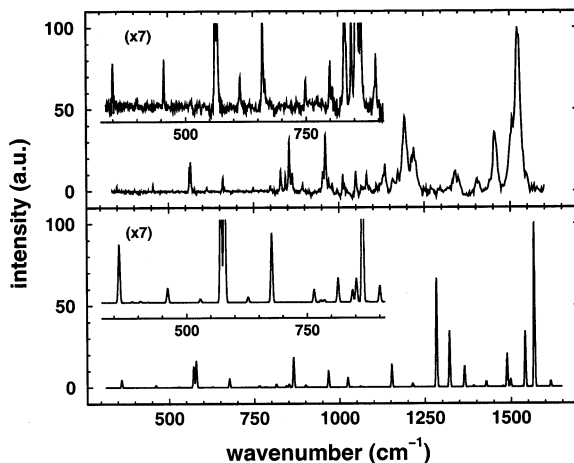

Fig. 6. Spectrum of cationic perdeuterated phenanthrene clustered with argon (upper panel) compared with the calculated spectrum of bare cationic perdeuterated phenanthrene (lower panel).
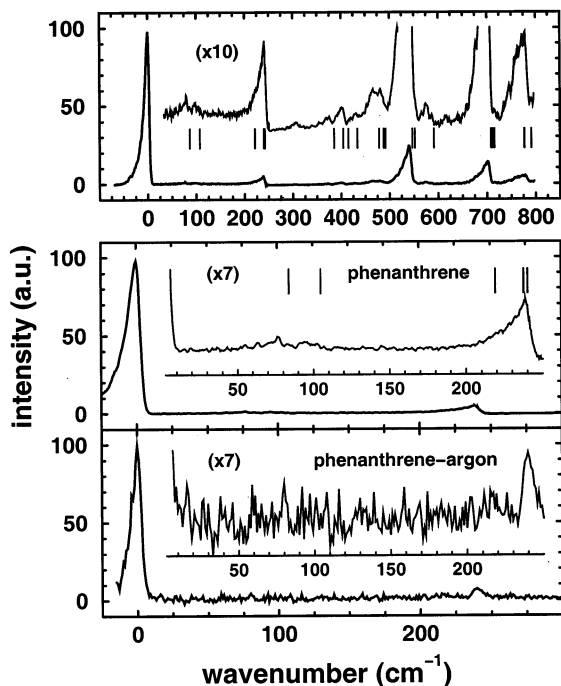
Fig. 7. MATI spectrum of phenanthrene (upper panel and middle panel) compared with that of the phenanthrene–argon Van der Waals cluster (lower panel). In the upper and the middle panel, the fundamental vibrational frequencies of the ion are indicated with bars.

5.2. Neutral phenanthrene

In Fig. 9, the cluster dissociation spectrum of neutral phenanthrene–Ar is presented, and compared with a calculated spectrum of neutral bare phenanthrene. In contrast with the spectrum of cationic phenanthrene–Ar, the neutral spectrum agrees well with the calculated IR spectrum. The positions of the two most prominent lines have also been recorded in neutral bare phenanthrene. Using IR-UV-REMPI, small ionization cross-sections and non-linear IR absorption behavior with respect to the IR intensity result in weak ion signals prohibiting recording of more lines of the neutral bare species. Within experimental errors, the line positions are the same as those of the Van der Waals cluster. After application of a linear correction for the IR fluence, the intensity ratio
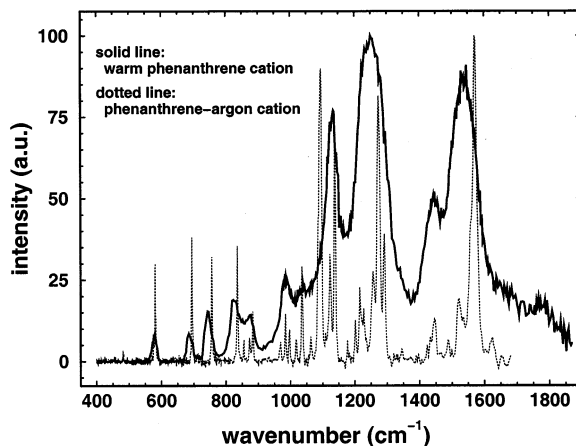

Fig. 8. Spectrum of cationic warm phenanthrene (solid line) compared with the observed spectrum of jet-cooled cationic phenanthrene clustered with argon (dotted line).

(100/80) between both lines observed differs significantly from that (100/37) observed in the cluster dissociation spectrum, which is clearly seen in Fig. 10.
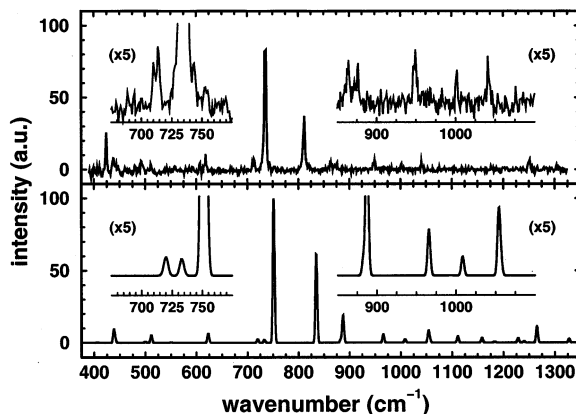

Fig. 9. The IR spectrum of neutral phenanthrene as observed with the cluster dissociation method (upper panel) compared with a calculated spectrum of neutral bare phenanthrene (lower panel). In the calculated spectrum all lines are convoluted with a 5 cm^{-1} (FWHM) Gaussian line shape. The band shown at ∼980 cm^{-1} in the calculated spectrum consists of two lines, which results in an asymmetric line shape.
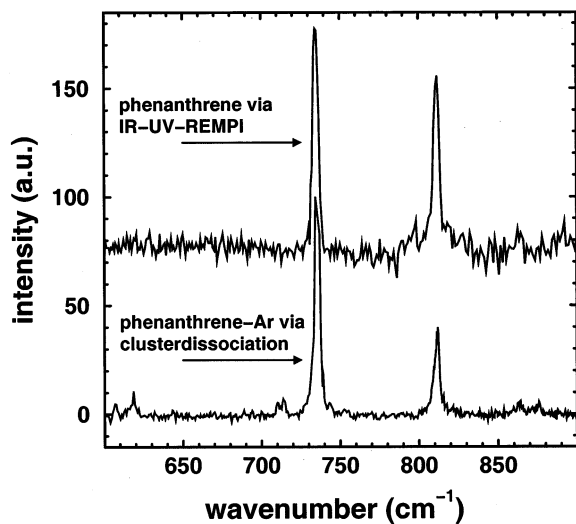
Fig. 10. IR-UV-REMPI spectrum of neutral phenanthrene compared with the observed photo-dissociation spectrum of neutral phenanthrene–Ar.

6. Discussion

6.1. The jet-cooled phenanthrene cation

Cationic phenanthrene–Ar data obtained via cluster dissociation spectroscopy are compared with MI spectroscopic data, observed in the 560–1580 cm^{-1} range. The paper [34] in which the MI spectral data of the phenanthrene cation has been presented originally, did not include the 850–1240 cm^{-1} region. However, as a result of the gas phase data presented here, Dr. D.M. Hudgins and coworkers have revisited [49] the MI measurements and have made available the newly obtained data, including bands in the 850–1240 cm^{-1} region. These data are given in Table 1 and Fig. 5 together with the gas phase data. It is seen that in the range studied, the line positions observed agree remarkably well. Relative intensities, however, differ, which can be explained by the low sensitivity of the direct absorption method used in MI experiments. For instance, the 581 cm^{-1} band is observed in the gas phase with a relative intensity of 31% of the strongest band, observed as a distinct peak at 1571 cm^{-1}, with a SNR of around 20. In the original MI experiment [34] this feature is observed as a $\sim 1\%$ baseline

depletion at 582 cm^{-1}, with a SNR of ~ 3, and a relative intensity of 22% of the strongest band, observed at 1565.0 cm^{-1} as a complex structure. In the 1240–1310 cm^{-1} range, the line shifts between MI and cluster dissociation spectra are somewhat larger.

The newly obtained MI spectral data in the 850–1240 cm^{-1} region, where the gas phase data differs most from the calculated IR spectrum, show a good match with the gas phase data when considering line positions. The relative intensities in this region are a factor three lower than observed in the gas phase data. Possible explanations for the discrepancies with the calculated spectra in this region will be discussed after discussion of all other data observed.

Comparison of gas phase perdeuterated cationic phenanthrene–Ar cluster data to MI spectral data [34], all tabulated in Table 2, again shows line shifts no larger than 5 cm^{-1} between data recorded via both types of experiments.

These very small shifts observed between spectra of phenanthrene cations embedded in an argon matrix and those of cations clustered with a single argon or neon atom, demonstrate that the interaction with the noble gas atom(s) is only very little. From the observed linear dependences on IR laser fluence at the 455 cm^{-1} resonance and the non-linear dependence on this fluence at the 349 cm^{-1} resonance, both of the perdeuterated cation, the Van der Waals bond energy of the argon atom in the cationic cluster is bracketed between these two energies. Thus, with an observed shift of the ionization threshold of the cluster compared with that of bare ionic phenanthrene of $\Delta IP \sim 65$ cm^{-1}, the dissociation energy D_0 of the neutral Van der Waals cluster can be bracketed between 284 $cm^{-1} < D_0 < 390$ cm^{-1}. This interval is in good agreement with earlier observed limits of the dissociation energies of aniline, benzene and naphthalene [41–43]. The low value of D_0 of the perdeuterated phenanthrene cation also indicates a minor interaction of the argon atom with the aromatic chromophore.

From the observed MATI data of bare phenanthrene and its Van der Waals cluster, all tabulated in Table 1, compared with the calculated fundamental modes of cationic phenanthrene, it is con-

cluded that in the 0–800 cm^{-1} region the MATI spectrum of bare phenanthrene agrees with the mode pattern calculated. Combining this observation with the observation of two low frequency modes of bare ionic phenanthrene at 78 and 239 cm^{-1}, which are also present in the MATI spectrum of the cluster, at 80 and 239 cm^{-1} and with similar intensities, respectively, confirms the earlier conclusion that in the frequency range below 800 cm^{-1}, the IR spectra observed via cluster dissociation behave like expected from calculations.

6.2. The warm phenanthrene cation

The photo-fragmentation spectrum of the warm phenanthrene cation shows an expected pattern. However, the intense peak showing up at 1095 cm^{-1} in the gas phase spectrum of the jet-cooled phenanthrene–Ar cation, cannot be recognized anymore in the spectrum of warm cationic phenanthrene. This spectrum is recorded starting from room temperature phenanthrene vapor. Therefore, after UV ionization the phenanthrene cations are at least as warm as room temperature. Sequential absorption of single IR photons at, slightly anharmonic, modes then happens between all $v' = n + 1 \leftarrow v'' = n$ transitions, if the $v'' = n$ state is populated in the warm ion. This causes the broad and little redshifted bands observed.

However, the absence of the 1095 cm^{-1} band in the spectrum of the warm cation, observed with high intensity in the spectrum of cold cationic phenanthrene is not explained well by this model. A possible explanation for the absent 1095 cm^{-1} band will also be included in the discussion of the 800–1400 cm^{-1} range at the end of this section.

6.3. Jet-cooled neutral phenanthrene

The spectral data of cluster dissociated neutral phenanthrene are also compared with MI data [37] and presented in Table 3. In MI experiments with neutral molecules, the SNR is much better than when observing cations in such experiments. Also the sensitivity is higher due to higher density of the species of interest, therefore, much more distinct lines are observed than in the cluster

dissociation experiment. However, the latter experiment shows two lines at 424 and 511 cm^{-1} that are not observed in MI experiments. Comparing line positions in both types of experiments, almost negligible shifts, all on the order of one wavenumber, are observed. Also, the relative intensities observed agree well in both types of experiments, except from the 812 cm^{-1} mode, which shows up with a significantly lower intensity (37% relative to the 735 cm^{-1} band) in the gas phase spectrum than in the MI spectrum (69% relative to the 735.0 cm^{-1} band). Comparing the line positions observed in the IR-UV-REMPI experiment to the cluster dissociation and MI data, again a negligible shift, within the experimental error, is observed at the two most prominent peaks indicating the interaction between the argon atom(s) and the aromatic chromophore to be very weak. The relative intensity of the 812 cm^{-1} mode is more than twice as high as in the case of cluster dissociation. A possible explanation for this difference could be a difference in UV ionization cross-section between the 735 cm^{-1} resonance and the 812 cm^{-1} resonance in the REMPI experiment. It is observed that the intensities in the UV-IR-REMPI spectrum scale with a more than linear dependence on the IR fluence, and that the ionization cross-section when ionizing from the 812 cm^{-1} resonance is different and larger than that when ionizing from the 735 cm^{-1} resonance.

6.4. The 900–1400 cm^{-1} spectral range of the phenanthrene cation

Focusing on the 900–1400 cm^{-1} spectral range of ionic phenanthrene, in which more modes and modes with different intensities are observed than expected from calculations, it is seen from Fig. 5 that, if IR forbidden transitions to modes with A2 character, present in this frequency region, are taken into account, enough fundamental modes exist to account for the anomalous structures, therefore, three possible explanations for these structures are discussed. (1) A symmetry lowering induced by the presence of the noble gas atom; (2) coupling of Van der Waals modes with fundamental modes of the chromophore, as is observed in

earlier work [58]; or (3) coupling of the fundamental groundstate vibrational modes of the chromophore with those of the first electronically excited state of the cation.

Obviously, the geometrical symmetry point group of the cluster cation is no longer C_{2v} as in the case of the bare cation. However, as a consequence of the low interaction between the noble gas atom and the aromatic chromophore, the vibrational wavefunctions do not have to be changed significantly due to the presence of this atom. In case the symmetries of the wavefunctions are lowered to the geometrical symmetry of the system, then the A_2 modes become IR active modes, and will be observed in an IR spectrum. However, this suggests that not only extra modes in the 900–1400 cm^{-1} should be observed, but also extra modes in the 400–900 cm^{-1} should be observable. Also the difference between either clustering with an argon atom or with a neon atom should be pronounced due to the much weaker interaction of neon with the aromatic chromophore than that of argon. In the spectrum of the perdeuterated phenanthrene cation, extra structures at lower frequencies should have been observed as well. A lowering of symmetry should also be present in the neutral cluster, leading to similar spectroscopic changes in the spectrum of neutral phenanthrene, which are not observed. Also, formerly recorded spectra of smaller aromatic systems, i.e. aniline, benzene and naphthalene, show no evidence of symmetry lowering due to the presence of a noble gas atom, not even when delicate interactions, like the Jahn–Teller interaction in benzene, are present [41–43]. From these arguments, it seems unlikely that a lowering of the C_{2v} symmetry is the origin of the anomalous structures observed in the 900–1400 cm^{-1} region.

Earlier experiments [58] on aromatic Van der Waals clusters show that anomalous line shifts, due to interaction of Van der Waals modes with fundamental vibrations of the chromophore in Van der Waals clusters, can occur, when comparing cluster spectra to those of the bare aromatic species. However, these anomalies observed are only limited to a few specific modes per molecule and seem to have no effect on other fundamental modes. They also depend strongly on the kind of noble gas atom present in the Van der Waals cluster. In the spectra of cationic phenanthrene–Ar and –Ne clusters, anomalies are observed in a wide frequency range. Clustering with an argon atom should also yield a different spectrum than when clustering with a neon atom, which is not observed. Also, anomalies should be observed at lower frequencies or be absent in the spectrum of cationic perdeuterated phenanthrene. However, in this latter spectrum, the anomalies present are observed in almost the same (800–1300 cm^{-1}) range, as is the case with cationic hydrogenated phenanthrene. The structures observed in the cluster dissociation spectra of cationic phenanthrene seem not to be consistent with anomalous shifts caused by interaction of fundamental vibrational modes with Van der Waals modes, therefore, it is concluded that these structures are not induced by this kind of interaction.

In photo-electron spectroscopy experiments, it is observed that the phenanthrene cation exhibits a very low lying first electronically excited state [77]. This state is present at an energy level comparable to those of the phenanthrene ionic fundamental vibrational modes, however, its position is not known with high accuracy. In cases like this, assuming coupling between vibrational states of the groundstate with those of the electronically excited state is reasonable. The calculations that we have conducted all start from the Born–Oppenheimer approximation, i.e. interaction between vibrational and electronic states is neglected, therefore, it is not surprising that, whenever a low lying electronic state exists at an energy level comparable to the vibrational energy levels, like in the case of cationic phenanthrene, calculations fail. Also the fact that in the perdeuterated cation anomalies are observed in the same range as in the hydrogenated case can be explained in this picture. Assuming only shifts in electronically excited states, due to zero point energy shifts upon deuteration, the shifts of electronically excited states are limited to tens of wavenumbers. This is inferred from the shifts observed in bare neutral phenanthrene (~ 90 cm^{-1} for the $S_1 \leftarrow S_0$ transition, and an IP shift of ~ -33 cm^{-1}, our observations). The region where coupling is observed in

the hydrogenated species, then should be almost the same as that of the perdeuterated species, which is in agreement with the IR spectra recorded. Since in the neutral molecule, no low lying electronically excited state exists, also the good agreement of the IR spectrum of neutral phenanthrene with the calculated spectrum is thus explained.

The absence of the 1095 cm^{-1} band in the spectrum of the warm cation can also be understood from the viewpoint of an existing low lying electronically excited state. Potential energy scans of several normal modes around 1000 cm^{-1} conducted with Gaussian 98, show almost harmonic vibrational potentials. Although the absence of the 1095 cm^{-1} band can be explained by a strongly anharmonic vibrational potential, it seems a little doubtful to assume one mode out of all to be so anharmonic, without further arguments, for instance given by the geometrical structure. However, if coupling between the first electronically excited state and the vibrational manifold of the groundstate cation exists, significant intensity changes and line shifts may occur. Still, two other strong bands in the affected region are readily observed in the spectrum of the warm cation. Realizing that in the warm cation IR transitions are induced mainly between vibrationally excited states, it is well possible that at room temperature the initial vibrational states are already excited around or above the first electronically excited state. This could mean that the 1095 cm^{-1} band, which behaves obviously differently in the warm cation than all other modes observed, already involves an electronic transition. The absence of this band then can be explained by coupling between the ground vibrational mode with modes of the first electronically excited state in combination with the different spacing of vibrational modes in this first electronically excited state, with respect to those of the cationic ground state. In this case, transitions starting from initially differently excited vibrational levels of the electronic cationic groundstate to the vibrational states of the first electronically excited state of the cation do not add up around a central frequency anymore. However, to draw firm conclusions on this idea, more experimental data together with

calculations at a higher level than B3LYP, which take into account the vibrational–electronical interaction between states, are needed.

7. Conclusions

The rich vibrational spectrum of neutral and cationic phenanthrene and that of cationic perdeuterated phenanthrene has been studied extensively, by means of photo-dissociation of their Van der Waals clusters, MATI spectroscopy and photofragmentation spectroscopy, in the case of the cation, and photo-dissociation of their Van der Waals clusters and IR-UV-REMPI, in the case of the neutral species. Comparison of the IR spectra of cold species observed with each other and with MI spectra show only minor differences in line positions and line intensities, which is also confirmed by the MATI spectra of phenanthrene and phenanthrene–Ar. This is in agreement with the results of earlier studies conducted on other molecules [42,55]. The spectrum of the warm cation shows an expected behavior, however, one major peak, present in the spectrum of cold phenanthrene cannot be recognized in that of the warm cation. Also, the calculated IR spectrum of the cation is not in good agreement with the observations. It is discussed that interference with a low lying electronically excited state gives a probable explanation for the discrepancy between the observed and calculated spectra. The experiments conducted demonstrate the cluster dissociation method to be a powerful method to obtain IR spectroscopic data of bare neutral and cationic jet-cooled species. Due to the only minor differences with MI data, observed in these experiments and in earlier experiments, it is concluded that in general, the unknown matrix interaction with vibrational modes of PAHs is almost negligible. Standard calculations of IR spectroscopical data alone cannot be used as a safe basis for drawing rigorous conclusions on the origin of the UIRs. IR spectra of PAHs can differ significantly from these calculations and can be more complex due to unexpected interactions, not accounted for in calculations.

Acknowledgements

References

[1] K. Sellgren, ApJ 277 (1984) 632.

[2] A. Léger, J.L. Puget, A&A 137 (1985) L5.

[3] L.J. Allamandola, A.G.G.M. Tielens, J.R. Barker, ApJ 290 (1985) L25.

[4] L.J. Allamandola, A.G.G.M. Tielens, J.R. Barker, ApJS 71 (1989) 733.

[5] M.L. Heger, Lick Obs. Bull. 10 (1922) 146.

[6] P.W. Merrill, Pub. A.S.P. 46 (1934) 206.

[7] G.H. Herbig, ApJ 196 (1975) 129.

[8] F.C. Gillett, W.J. Forrest, K.M. Merrill, ApJ 183 (1973) 87.

[9] R. Papoular, J. Conard, M. Giuliano, J. Kister, G. Mille, A&A 217 (1989) 204.

[10] A. Sakata, S. Wada, T. Tanabe, T. Onaka, ApJ 287 (1984) L51.

[11] A. Sakata, S. Wada, T. Onaka, A.T. Tokunaga, ApJ 320 (1987) L63.

[12] A. Sakata, S. Wada, T. Onaka, A.T. Tokunaga, ApJ 353 (1990) 543.

[13] D.M. Hudgins, L.J. Allamandola, S.A. Sandford, Adv. Space Res. 19 (1997) 999.

[14] S. Leach, in: A. Léger, L.B. d'Hendecourt, N. Boccara (Eds.), Polycyclic Aromatic Hydrocarbons and Astrophysics, Reidel, Dordrecht, 1987, p. 99.

[15] S. Leach, J. Electron Spectrosc. Rel. Phen. 41 (1987) 427.

[16] H.W. Jochims, E. Ruhl, H. Baumgartel, S. Tobita, S. Leach, ApJ 420 (1994) 307.

[17] H.W. Jochims, H. Baumgartel, S. Leach, A&A 314 (1996) 1003.

[18] L. d'Hendecourt, E. Dartois, in: E.Y. van Dishoeck (Ed.), Molecules in Astrophysics: Probes and Processes, IAU, 1997, p. 362.

[19] T. Allain, S. Leach, E. Sedlmayr, A&A 305 (1996) 602.

[20] T. Allain, S. Leach, E. Sedlmayr, A&A 305 (1996) 616.

[21] S.P. Ekern, A.G. Marshall, J. Szczepanski, M. Vala, J. Phys. Chem. A 102 (1998) 3498.

[22] D.J. Cook, S. Schlemmer, N. Balucani, D.R. Wagner, B. Steiner, R.J. Saykally, Nature 380 (1996) 227.

[23] D.J. Cook, S. Schlemmer, N. Balucani, D.R. Wagner, J.A.D.R. Harrison, B. Steiner, R.J. Saykally, J. Phys. Chem. 102 (1998) 1465.

[24] J. Szczepanski, D. Roser, W. Personette, M. Eyring, R. Pellow, M. Vala, J. Phys. Chem. 96 (1992) 7876.

[25] D.M. Hudgins, L.J. Allamandola, S.A. Sandford, J. Phys. Chem. 98 (1994) 4243.

[26] D.J. DeFrees, M.D. Miller, in Interstellar Dust: Contributed Papers, L.J. Allamandola and A.G.G.M. Tielens (Eds.), NASA CP 3036 1989, p. 173.

[27] J. Szczepanski, M. Vala, Nature 363 (1993) 699.

[28] J. Szczepanski, M. Vala, ApJ 414 (1993) 646.

[29] J. Szczepanski, C. Chapo, M. Vala, Chem. Phys. Lett. 205 (1993) 434.

[30] J. Szczepanski, M. Vala, D. Talbi, O. Parisel, Y. Ellinger, J. Chem. Phys. 98 (1993) 4494.

[31] J. Szczepanski, C. Wehlburg, M. Vala, Chem. Phys. Lett. 232 (1995) 221.

[32] J. Szczepanski, J. Drawdy, C. Wehlburg, M. Vala, Chem. Phys. Lett. 245 (1995) 539.

[33] M. Vala, J. Szczepanski, F. Pauzat, O. Parisel, D. Talbi, Y. Ellinger, J. Phys. Chem. 98 (1994) 9187.

[34] D.M. Hudgins, L.J. Allamandola, J. Phys. Chem. 99 (1995) 3033.

[35] D.M. Hudgins, L.J. Allamandola, J. Phys. Chem. 99 (1995) 8978.

[36] D.M. Hudgins, L.J. Allamandola, J. Phys. Chem. A 101 (1997) 3472.

[37] D.M. Hudgins, S.A. Sandford, J. Phys. Chem. A 102 (1998) 329.

[38] D.M. Hudgins, S.A. Sandford, J. Phys. Chem. A 102 (1998) 344.

[39] D.M. Hudgins, S.A. Sandford, J. Phys. Chem. A 102 (1998) 353.

[40] C.W. Bauschlicher, Jr, S.R. Langhoff, S.A. Sandford, D.M. Hudgins, J. Phys. Chem. A 101 (1997) 2414.

[41] J.A. Piest, G. von Helden, G. Meijer, J. Chem. Phys. 110 (1999) 2010.

[42] J.A. Piest, G. von Helden, G. Meijer, ApJ 520 (1999) L75.

[43] R.G. Satink, J.A. Piest, G. von Helden, G. Meijer, J. Chem. Phys. 111 (1999) 10750.

[44] K. Remmers, R.G. Satink, G. von Helden, J.A. Piest, G. Meijer, W.L. Meerts, Chem. Phys. Lett. 317 (2000) 197.

[45] P. Bréchignac, T. Pino, A&A 343 (1999) L49.

[46] T. Pino, N. Boudin, Ph. Bréchignac, J. Chem. Phys. 111 (1999) 7337.

[47] M. Putter, G. von Helden, G. Meijer, Chem. Phys. Lett. 258 (1996) 118.

[48] A. Fujii, E. Fujimaki, T. Ebata, N. Mikami, Chem. Phys. Lett. 303 (1999) 289.

[49] D.M. Hudgins, NASA-AMES Research Center, Moffett Field, CA, USA, private communications.

[50] M. Okumura, L.I. Yeh, Y.T. Lee, J. Chem. Phys. 83 (1985) 3705.

[51] M. Okumura, L.I. Yeh, J.D. Myers, Y.T. Lee, J. Phys. Chem. 94 (1990) 3416.

[52] R.N. Pribble, T.S. Zwier, Science 265 (1994) 75.

[53] O. Dopfer, D. Roth, R.V. Olkhov, J.P. Maier, J. Chem. Phys. 110 (1999) 11911.

[54] K. Kleinermanns, Ch. Janzen, D. Spangenberg, M. Gerhards, J. Phys. Chem. A 103 (1999) 5232.

[55] O. Dopfer, D. Roth, R.V. Olkhov, J.P. Maier, J. Chem. Phys. 111 (1999) 10754.

[56] W.E. Henke, Weijun Yu, H.L. Selzle, E.W. Schlag, D. Wutz, S.H. Lin, Chem. Phys. 92 (1985) 187.

[57] T. Vondrák, S. Sato, K. Kimura, Chem. Phys. Lett. 261 (1996) 481.

[58] B. Coutant, P. Bréchignac, J. Chem. Phys. 100 (1994) 7087.

[59] D. Oepts, A.F.G. van der Meer, P.W. van Amersfoort, Infrared Phys. Technol. 36 (1995) 297.

[60] G.M.H. Knippels, R.F.X.A.M. Mols, A.F.G. van der Meer, D. Oepts, P.W. van Amersfoort, Phys. Rev. Lett. 75 (1995) 1755.

[61] M.G.H. Boogaarts, G. von Helden, G. Meijer, J. Chem. Phys. 105 (1996) 8556.

[62] W.C. Wiley, I.H. McLaren, Rev. Sci. Instru. 26 (1955) 1150.

[63] T. Troxler, R. Knochenmuss, S. Leutwyler, Chem. Phys. Lett. 159 (1989) 554.

[64] L. Zhu, P. Johnson, J. Chem. Phys. 94 (1991) 5769.

[65] D. Bahatt, U. Even, R.D. Levine, J. Chem. Phys. 98 (1993) 1744.

[66] W.A. Chupka, J. Chem. Phys. 99 (1993) 5800.

[67] F. Merkt, R.N. Zare, J. Chem. Phys. 101 (1994) 3495.

[68] P.M. Felker, A.H. Zewail, J. Chem. Phys. 82 (1995) 2975.

[69] Y. Gotkis, M. Oleinikova, M. Naor, C. Lifshitz, J. Phys. Chem. 97 (1993) 12282.

[70] J. Oomens, A.J.A. van Roij, G. Meijer, G. von Helden, ApJ, 542 (2000) 404.

[71] W. Paul, Rev. Mod. Phys. 62 (1990) 531.

[72] T.H. Dunning, Jr, P.J. Hay, in: H.S. Schäfer, III (Ed.), Modern Theoretical Chemistry, Plenum, New York, 1976.

[73] M.J. Frisch, G.W. Trucks, H.B. Schlegel, G.E. Scuseria, M.A. Robb, J.R. Cheeseman, V.G. Zakrzewski, J.A. Montgomery Jr., R.E. Stratmann, J.C. Burant, S. Dapprich, J.M. Millam, A.D. Daniels, K.N. Kudin, M.C. Strain, O. Farkas, J. Tomasi, V. Barone, M. Cossi, R. Cammi, B. Menucci, C. Pomelli, C. Adamo, S. Clifford, J. Ochterski, G.A. Petersson, P.Y. Ayala, Q. Cui, K. Morokuma, D.K. Malick, A.D. Rabuck, K. Raghavachari, J.B. Foresman, J. Cioslowski, J.V. Ortiz, B.B. Stefanov, G. Liu, A. Liashenko, P. Piskorz, I. Komaromi, R. Gomperts, R.L. Martin, D.J. Fox, T. Keith, M.A. Al-Laham, C.Y. Peng, A. Nanayakkara, C. Gonzalez, M. Challacombe, P.M.W. Gill, B. Johnson, W. Chen, M.W. Wong, J.L. Andres, C. Gonzalez, M. Head-Gordon, E.S. Replogle, J.A. Pople, Gaussian 98, Revision A.5, Gaussian, Inc., Pittsburgh PA, 1998.

[74] S.R. Langhoff, J. Phys. Chem. 100 (1996) 2819.

[75] N. Ohta, H. Baba, Mol. Phys. 59 (1986) 921.

[76] C. Joblin, P. Boissel, A. Léger, L. d'Hendecourt, D. Défourneau, A&A 299 (1995) 835.

[77] W. Schmidt, J. Chem. Phys. 66 (1977) 828.